Synthesis of 1.4 nm α-Cyclodextrin-Protected Gold Nanoparticles for Luminescence Sensing of Mercury(II) with Picomolar Detection Limit†

ARTICLE *in* THE JOURNAL OF PHYSICAL CHEMISTRY C · APRIL 2010

Impact Factor: 4.77 · DOI: 10.1021/jp101571k

4 AUTHORS, INCLUDING:

Xiupei Yang
China West Normal University
28 PUBLICATIONS **407** CITATIONS

SEE PROFILE

Synthesis of 1.4 nm α-Cyclodextrin-Protected Gold Nanoparticles for Luminescence Sensing of Mercury(II) with Picomolar Detection Limit†

Man Chin Paau,[‡] Chung Keung Lo,[‡,||] Xiupei Yang,[§,⊥] and Martin M. F. Choi*[,‡]

Department of Chemistry, Hong Kong Baptist University, 224 Waterloo Road, Kowloon Tong, Hong Kong SAR, People's Republic of China, and College of Chemistry and Chemical Engineering, China West Normal University, Nanchong 637002, People's Republic of China

Received: February 22, 2010; Revised Manuscript Received: April 10, 2010

The synthesis of gold nanoparticles (core size less than 2.0 nm) capped by thiolate α-cyclodextrin (α-CD-SH) has been studied and characterized by infrared spectroscopy, UV−visible absorption spectroscopy, high-resolution transmission electron microscopy, and photoluminescence spectroscopy. Hydrogen tetrachloroaurate(III) trihydrate ($HAuCl_4•3H_2O$) is reduced by $NaBH_4$ in the presence of α-CD-SH to produce thiolate α-cyclodextrin-stabilized gold nanoparticles (α-CD-S-AuNPs). The particle size of the as-synthesized α-CD-S-AuNPs is highly dependent on the initial molar ratio of α-CD-SH to $AuCl_4^-$ (α-CD-SH/Au) precursors. When the α-CD-SH/Au is kept greater than or equal to 1, α-CD-S-AuNPs (core size < 2.0 nm) are acquired, and their size increases with increasing α-CD-SH/Au. It is postulated that the increase in particle size is attributed to the interhydrogen bond between the α-CD-SH molecules at higher concentrations with a concomitant decrease in the availability of free α-CD-SH to stabilize the AuNP surface. By contrast, when the α-CD-SH/Au is controlled at <1, larger α-CD-S-AuNPs (core size >2.5 nm) with typical surface plasmon bands are obtained, and the particle size increases with the decrease in α-CD-SH/Au. The average chemical compositions of such AuNPs in the empirical formula $Au_x(α\text{-CD-S})_y$ are further determined by thermogravimetric analysis, mass spectrometry, and atomic absorption spectroscopy. These α-CD-S-AuNPs (core size < 2.0 nm) display remarkably strong blue emissions at 478 nm when excited at 400 nm. The 1.4 nm-sized α-CD-S-AuNP shows photoluminescence enhancement in the presence of tetraalkylammonium ions but is strongly quenched by Hg(II). The α-CD-S-AuNP possesses ultrahigh sensitivity and good selectivity for the determination of Hg(II) with the limit of detection at 49 pM (9.7 ppt).

1. Introduction

Nanometer-sized particles are significantly interesting due to their various unique chemical and physical properties. Many important applications in the fields of catalysis, chemical sensing, electronic devices, optics, and biomedical applications are dependent on the size and shape of metal nanoparticles.[1] It is now possible to manipulate or even control the properties of metal colloidal particles by modifying their surfaces with a monolayer of organic molecules (ligands).[2] An attractive aspect of recent development is that gold nanoparticles (AuNPs) of 1−2 nm are almost somewhat molecule-like, and they possess interesting and size-dependent properties including optical absorption,[3] quantized electrical charging[4] and catalytic activity.[5] Previous works have demonstrated that alkanethiols,[6] tiopronin,[7] *N*-acetyl-L-cysteine,[8] homocysteine,[9] and many other organic molecules can be used to passivate AuNPs. The introduction of organic molecules on AuNPs surface not only stabilizes these nanoentities in different solvents but also provides the desired surface functionality.

Recently in modern nanochemistry research, the modification of AuNPs with multidentate functional molecules has been fruitful.[10] Cyclodextrins (CDs) are cyclic oligomers of six, seven, or eight glucose molecules. The outside of the CDs toroid is hydrophilic due to the hydroxyl groups, imparting the molecules with good water-solubility, whereas the interior is relatively hydrophobic because of the glycosidic oxygen bridges.[11] As such, CDs are regarded as a representative of the supramolecular host compounds used to functionalize the NPs as a result of their high water-solubility, low toxicity, and specific recognition ability toward many model substrates. Thiolate-modified CDs and other CD derivatives have been successfully chemisorbed onto Au surfaces. Most of these works were performed with β-CD, whereas some used α-CD derivatives.[12] In addition, the formation of inclusion complexes between ferrocene derivatives and CD hosts immobilized on the AuNPs was well studied by Kaifer's group.[13] They have demonstrated that thiolate β-cyclodextrin (β-CD-SH) receptors immobilized onto the surface of larger Au colloidal particles (12.5 nm diameter) maintained their host binding ability toward ferrocene dimers. They also reported clear electrochemical evidence on the binding of water-soluble ferrocenemethanol and 1-adamantanol to the CD-S-capped AuNPs (∼3 nm). The effect of $[\beta\text{-CD-SH}]/[AuCl_4^-] < 1$ on the size of AuNPs was investigated.[14] Similar work was also performed with simple alkanethiols.[15] Their group illustrated the binding interactions of AuNPs capped with thiolate α-CD and β-CD hosts with a series of five cationic ferrocene derivatives. These interactions can transfer the hydrophilic CD-

† Part of the special issue "Protected Metallic Clusters, Quantum Wells and Metallic Nanocrystal Molecules".

* Corresponding author. Fax: +852-34117348. E-mail: mfchoi@hkbu.edu.hk.

‡ Hong Kong Baptist University.

§ China West Normal University.

|| Current address: Waters China Limited, 102 Austin Road, Kowloon, Hong Kong.

⊥ Visiting Scholar to Hong Kong Baptist University.

10.1021/jp101571k
Published on Web 04/20/2010

modified NPs into low polarity solution phase.[13b] More recently, sulfur-modified α-CD derivatives without long alkyl chains have been used to prepare stable and orderly CD monolayers on Au, and its host−guest complexation has been studied by electrochemical capacitance measurements.[12d] Obviously, the binding ability of CD-S-AuNPs has been well recognized. Unfortunately, the effect of [α-CD-SH]/[$AuCl_4^-$] (α-CD-SH/A*u* ≥ 1) on AuNP particle size and composition of α-CD-S-AuNPs has not been investigated in detail. Furthermore, the photoluminescence (PL) properties of AuNPs have been recognized and applied in biosensors because of their dimensional similarities with biomacromolecules and significant size-dependent optical and electronic properties.[16] To our knowledge, the PL properties of CD-S-AuNPs and its application in Hg(II) sensing have not been studied.

In this work, the use of α-CD-SH/A*u* ≥ 1 to synthesize small-sized (core size <2.0 nm) AuNPs capped by α-CD-S ligand is reported. More specifically, our focus is to more thoroughly study the effect of α-CD-SH/Au on the core size of the as-synthesized α-CD-S-AuNPs. In contrast to most studies, we observe that when the α-CD-SH/Au is greater than 1, the core size of AuNPs increases with the increase in α-CD-SH/Au, which is just opposite to the trend obtained from α-CD/A*u* < 1. The results are well supported by UV−visible (UV−vis) absorption spectroscopy, high-resolution transmission electron microscopy (HRTEM), mass spectrometry (MS), thermogravimetric analysis (TGA), and atomic absorption spectrometry (AAS). The average chemical compositions of our synthesized α-CD-S-AuNPs have been determined as $Au_x(\alpha\text{-CD-S})_y$, where *x* is the number of Au atoms and *y* is the number of attached α-CD-S ligands. Our proposed methodology and the acquired data should provide useful information in the field of nanoscience for the synthesis of small CD-S-AuNPs and determination of their chemical composition. In addition, we first observe that these small α-CD-S-AuNPs also display strong blue emissions, which have potential applications in optical chemo/biosensors. These small α-CD-S-AuNPs also exhibit unusual enhancement in PL intensity via the interaction with tetraalkylammonium ion based on the aggregation-enhanced emission phenomenon. By contrast, it displays PL quenching in the presence of Hg(II). The small α-CD-S-AuNPs have been successfully applied to determine Hg(II) with ultrahigh sensitivity and excellent selectivity.

2. Experimental Section

2.1. Chemicals and Reagents. *N*,*N*-Dimethylformamide (DMF), glacial acetic acid, hydrogen tetrachloroaurate(III) trihydrate ($HAuCl_4 \cdot 3H_2O$ > 99.9%), mercury(II) acetate, potassium hydrogensulfate, sodium borohydride ($NaBH_4$, 99%), sodium methoxide, tetrabutylammonium (Bu_4N^+) bromide, tetraethylammonium (Et_4N^+) bromide, tetramethylammonium (Me_4N^+) bromide, and tetrapropylammonium (Pr_4N^+) bromide were purchased from Aldrich (Milwaukee, WI). 2,5-Dihydroxybenzoic acid (DHB, 98%), iodine, thiourea, and triphenylphosphine were from Sigma (St. Louis, MO). Acetone, dimethylsulfoxide (DMSO), ethanol (EtOH), and methanol (MeOH) of HPLC grade were purchased from Labscan (Bangkok, Thailand). Trisodium phosphate, hydrochloric acid (HCl), and sodium hydroxide (NaOH) were obtained from Farco Chemical Supplies (Beijing, China). Nitric acid (HNO_3) was purchased from BDH (Poole, England). Hydrofluoric acid (HF) was obtained from Riedel-da Haën (Seelze, Germany). Ammonia solution was purchased from Ajax Chemical (Auburn, Australia). α-CD was obtained from Acros Organics (Geel, Belgium). Dimethylsulfoxide-d_6 (DMSO-d_6) was purchased from Armar Chemicals (Dottingen, Switzerland). All reagents were of analytical grade or above. Water was purified by a Milli-Q-RO4 water purification system (Millipore, Bedford, MA). Distilled deionized (DDI) water was used unless otherwise stated.

2.2. Synthesis of α-CD-Modified AuNPs. The α-CD-SH ligand and its precursor per-6-iodo-α-cyclodextrin were synthesized as described in the Supporting Information. The synthetic procedures of α-CD-S-AuNP were similar to our previous work.[8] In a typical synthesis, 9.0 mg $HAuCl_4 \cdot 3H_2O$ and 24.4 mg α-CD-SH were codissolved in 2.0 mL of 6:1 v/v DMF/acetic acid, giving a yellow solution. After stirring for 30 min, $NaBH_4$ (80 mg) in 0.20 mL of EtOH was added with rapid stirring at room temperature (∼20 °C). The dark-brown suspension formed was stirred for an additional 24 h, and acetone was then added to precipitate the crude α-CD-S-AuNP product. The residues were collected by centrifugation. Then, it was purified by dialysis with the crude product dissolved in 30 mM phosphate buffer (pH 12). This solution was loaded into 24-mm flat width segments of Spectr/Por^R cellulose ester dialysis tubes (Spectrum Laboratories, Rancho Dominguez, CA) and placed in a 1 L beaker of 30 mL phosphate buffer (pH 12) over the course of 7 days. The dark-brown α-CD-S-AuNP solutions were collected from the dialysis tubes, and excess amounts of HCl were added to precipitate the product, which was then collected by centrifugation. This product was washed by DDI water until the supernatant fluid was neutral and dried in a Virtis freeze-drier (Gardiner, NY). The above preparation procedures for synthesizing α-CD-S-AuNP were based on a 1:1 α-CD-SH/Au molar ratio. Other α-CD-S-AuNPs synthesized with different α-CD-SH/Au molar ratios and constant [$AuCl_4^-$] were also prepared.

2.3. Characterization. All UV−visible absorption spectra were acquired with a Varian Cary 300 Scan UV−visible absorption spectrophotometer (Palo Alto, CA) over the wavelength range from 220 to 800 nm. The PL properties of α-CD-S-AuNPs were recorded by a PTI QM4 spectrofluorometer (Lawrenceville, NJ). All the α-CD-S-AuNPs solutions for spectral studies were prepared in DMSO. Infrared (IR) spectra were acquired with a Perkin-Elmer Paragon 1000 FTIR spectrometer (Waltham, MA). The α-CD-S-AuNP sample was mixed with KBr and ground into fine powders. The powders were pressed into a pellet at 15000 psi. The IR spectra were collected over the range of 500−4000 cm^{-1}. ^1H NMR spectra were recorded on a Varian 400 MHz FT-NMR Spectrometer Inova 400 (Palo Alto, CA). Samples (2.0 mg) were dissolved in 0.5 mL DMSO-d_6 for measurements.

TEM and HRTEM images of α-CD-S-AuNP samples were acquired with a Philips CM 20 TEM and a JEOL JEM-2010 HRTEM operating at 200 kV, respectively. Sample was prepared by casting and evaporating a droplet of EtOH/H_2O (9:1 v/v) solution of α-CD-S-AuNP onto an Agar Scientific 300-mesh holey carbon-coated copper grid (Stansted, Essex, U.K.).

The α-CD-S-AuNP samples synthesized with different α-CD/Au ratios were analyzed by an Autoflex matrix-assisted laser desorption/ionization time-of-flight mass spectrometer (MALDI-TOF MS) (Bruker-Daltonics, Bremen, Germany). The sample was dissolved in an ammonia solution (ca. pH 11) and then mixed in 1:1 v/v with a 1.0 M solution of DHB in MeOH/H_2O (1:1 v/v). 5.0 μL of this solution was deposited on a MALDI target plate and air-dried. The sample was irradiated by a pulsed N_2 laser at 337 nm, and the laser intensity was minimized to avoid excessive AuNP fragmentation.

The weight percentages of α-CD-S on α-CD-S-AuNP samples synthesized with various α-CD-SH/Au molar ratios were determined by a Perkin-Elmer TGA 6 thermogravimetric analyzer (Waltham, MA). About 3.0 mg of the α-CD-S-AuNP sample was put into a ceramic pan, and the temperature was ramped from room temperature to 400 °C at a heating rate of 10 °C/min. Finally, the Au compositions of α-CD-S-AuNP samples were determined by a Varian Spectra AA 220FS atomic absorption spectrometer (Mulgrave, Victoria, Australia). First, samples were sequentially digested by aqua regia (3:1 v/v HCl/HNO_3) and then HF in a CEM MARS 5 microwave oven (Matthews, NC). Then, the samples were diluted to Au concentrations in the range of 0.50−2.5 μM for AAS analysis. Calibration curves were made from the dilution of Au standards with 0.50−2.5 μM in the same acid matrices as the samples. AAS measurements were made at 242.8 nm under air−acetylene flames for Au analysis.

3. Results and Discussion

The α-CD-capped AuNPs were formed by reduction of $HAuCl_4$ with $NaBH_4$ in a solvent mixture of 6:1 v/v DMF/acetic acid containing α-CD-SH. The attachment of thiolate CDs to AuNPs can be verified by IR spectroscopy.[17] The IR spectrum of 1.4 nm-sized α-CD-S-AuNP shows similar bands to free α-CD-SH (Figure S1 in the Supporting Information), demonstrating that the α-CD-S− moiety is a constituent of the ligand shell. The peak at 2560 cm^{-1} (S−H stretching mode vibration) for the α-CD-S-AuNP sample vanished, indicating that the −SH groups were consumed during the formation of AuNP. Hence, the modification of AuNP with α-CD-SH can be confirmed.[17c,d] One of the aims of this work is to investigate the effect of α-CD-SH/Au on the core size of AuNP. Measurements on the NP preparations were conducted with a combination of analytical tools, including TEM and HRTEM for Au core size, MALDI-TOF MS for AuNP mass, TGA for thiolate α-CD coverage, and AAS for Au atom. The results of these measurements are remarkably consistent and will be discussed in the subsequent sections.

3.1. UV−Vis Analysis. UV−vis absorption spectroscopy has been a potent tool in the preliminary study of the size of AuNPs. Small core Au clusters exhibit a strong UV absorption feature, which decays approximately exponentially into the visible region with a superimposed broad band (surface plasmon (SP) resonance band) at ∼500 nm.[7,18] The SP band wavelength and intensity decrease with decreasing cluster size.[19] As such, the optical properties of Au clusters have been the subject of several papers.[20] In addition, UV−vis absorption spectrometers are present in most laboratories, the analysis does not alter the sample, and the registration of spectrum requires short times. Therefore, UV−vis absorption spectroscopy has been utilized to give a fundamental evaluation of the average size trend of the separated AuNPs in our recent articles.[8] The effect of various α-CD-SH/Au molar ratios, i.e., 3:1, 2:1, 1:1, 1:3, 1:5, and 1:10 on the α-CD-S-AuNP products were determined by their UV−vis absorption spectra as depicted in Figure 1. These spectra are normalized at 220 nm to remove the effect of concentration differences to allow comparison of spectral shape and band position. The differences in the normalized absorption spectra of the AuNPs well demonstrate the change in particle size under different α-CD-SH/Au molar ratios. The spectral profiles of α-CD-S-AuNP with α-CD-SH/Au < 1 (i.e., 1:3, 1:5 and 1:10) exhibit typical SP bands in the visible region (∼519−540 nm) in addition to the otherwise smooth exponential-like curves. In essence, the wavelength of SP band is clearly dependent on particle size. The larger the particle size, the more red-shift the wavelength. The hump (SP band in Figure 1) indicated by the arrow tends to be bathochromatically shifted and gradually broadens with decreasing α-CD-SH/Au, inferring that the AuNP size increases with the decrease in α-CD-SH/Au.[17d] This can be explained by the fact that there are not enough free α-CD-SH ligands to bind on the AuNP surface to prevent the Au atoms from coalescence and aggregation. The spectral characteristics of α-CD-S-AuNP prepared with α-CD-SH/Au < 1 are in complete agreement with the previous AuNP spectra.[15,17d,18]

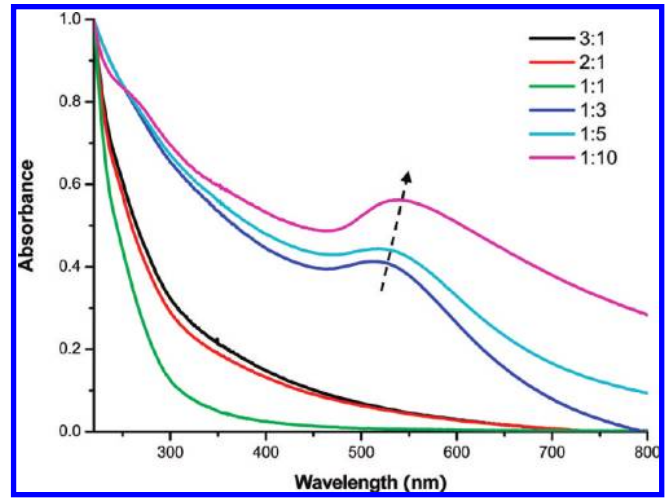

Figure 1. UV−vis absorption spectra of α-CD-S-AuNP synthesized with different molar ratios of α-CD-SH/Au: 3:1, 2:1, 1:1, 1:3, 1:5, and 1:10. The arrow indicates the bathochromic shift of the SP band with the increase in the size of AuNP. The spectra are normalized at 220 nm for ease of comparison.

To our surprise, the spectral profiles of α-CD-S-AuNP synthesized with α-CD-SH/Au ≥ 1, i.e., 3:1, 2:1 and 1:1 are in sharp contrast to that prepared with α-CD-SH/Au < 1. Their spectral decay in approximately an exponential fashion into the visible region with no discernible SP band suggests that these α-CD-S-AuNPs have core diameters smaller than that of those prepared with α-CD-SH/Au < 1, which is larger than 2 nm. Earlier studies[7,15,18] and our previous work[8] showed that smaller core AuNPs possess a sharper decrease in absorbance than that of larger core AuNPs from shorter to longer wavelengths. Smaller core AuNP also produces an absorption spectrum with relatively lower absorbance than that of larger core AuNP in the visible region. In summary, when the α-CD-SH/Au is ≥1, increasing the α-CD-SH/Au will produce a larger AuNP. By contrast, when the α-CD-SH/Au is <1, increasing the α-CD-SH/Au will result in a smaller AuNP. These results are further confirmed by TEM, HRTEM and MALDI-TOF MS analyses (*vide infra*).

3.2. HRTEM Analysis. TEM can provide crucial information on the size and dispersity of thiolate CD-capped AuNPs.[21] Liu et al.[13b] reported that the nature of the perthiolate CD can also affect the particle size of the final modified AuNP. Traditionally, CD-S-AuNPs with larger core sizes (>2.0 nm) are usually prepared with CD-SH/Au < 1. For instance, a 1:5 β-CD-SH/Au yielded NPs with an average diameter of 2.9 ± 0.7 nm, while a higher α-CD-SH/Au of 1:4 had to be used to obtain NPs of similar sizes (diameter = 3.1 ± 0.7 nm) as a reflection of less thiol units in the latter host. To our surprise, the synthesis of small (core Au < 2.0 nm) α-CD-S-AuNPs has not been reported in literature so far. However, they have attracted considerable attention recently for their unique optical

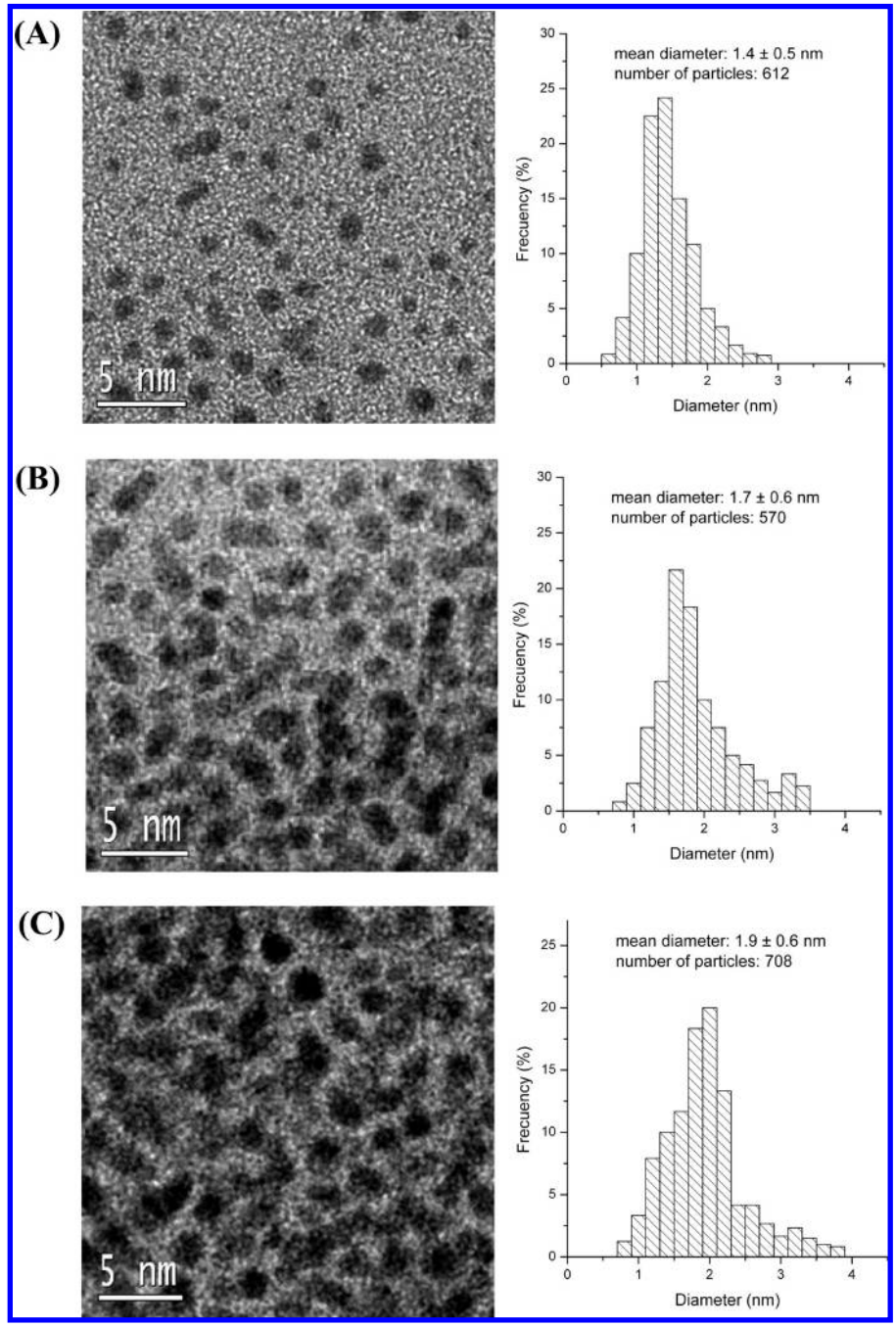

Figure 2. HRTEM images and core size histograms of α-CD-S-AuNPs synthesized with different molar ratios of α-CD-SH/Au: (A) 1:1, (B) 2:1, and (C) 3:1.

and electrochemical properties. In the 1−2 nm core size range, the electronic properties of NPs possess molecule-like discrete electronic orbital levels as opposed to the bulk-like continuum electronic states of the larger NPs. Also, it is more likely to observe the interesting PL properties of small AuNPs in the visible/near-infrared regions.

Figure 2A−C displays the HRTEM images of α-CD-S-AuNPs synthesized with 1:1 (diameter = 1.4 ± 0.5 nm), 2:1 (diameter = 1.7 ± 0.6 nm), and 3:1 (diameter = 1.9 ± 0.6 nm) α-CD-SH/Au molar ratios, respectively. For comparison, larger core sizes (>2.0 nm) of α-CD-S-AuNP were also synthesized by using α-CD-SH/Au < 1 in this work. Compared with the findings in previous literature,[12a,13b] our TEM results on the size of α-CD-S-AuNPs shown in Figure S2 are reasonable. The representative TEM images in Figure S2A−C provide solid evidence that the average AuNP core size decreases progressively from 4.1 ± 0.9 nm to 3.5 ± 0.7 nm, and then to 2.7 ± 0.7 nm according to the α-CD-SH/Au 1:10, 1:5, and 1:3, respectively. It has been reported that unmodified CDs exhibit hydrophobic interactions with embryonic AuNPs.[22] The consecutive particle growth due to mutual coalescence between NPs would be limited or terminated as the CD concentration increases.[23] Our results are consistent with other findings that larger thiol/Au in the synthetic process produces smaller average NP core size.[24] The effect of α-CD-SH on AuNPs size recorded by HRTEM and TEM agrees well to that determined by UV−vis analysis (*vide supra*). On the other hand, the smallest particles were obtained at 1:1 α-CD-SH/Au (diameter = 1.4 ± 0.5 nm) rather than the higher α-CD-SH/Au. Interestingly, further increase of α-CD-SH/Au (≥1) results in the formation of larger particles.

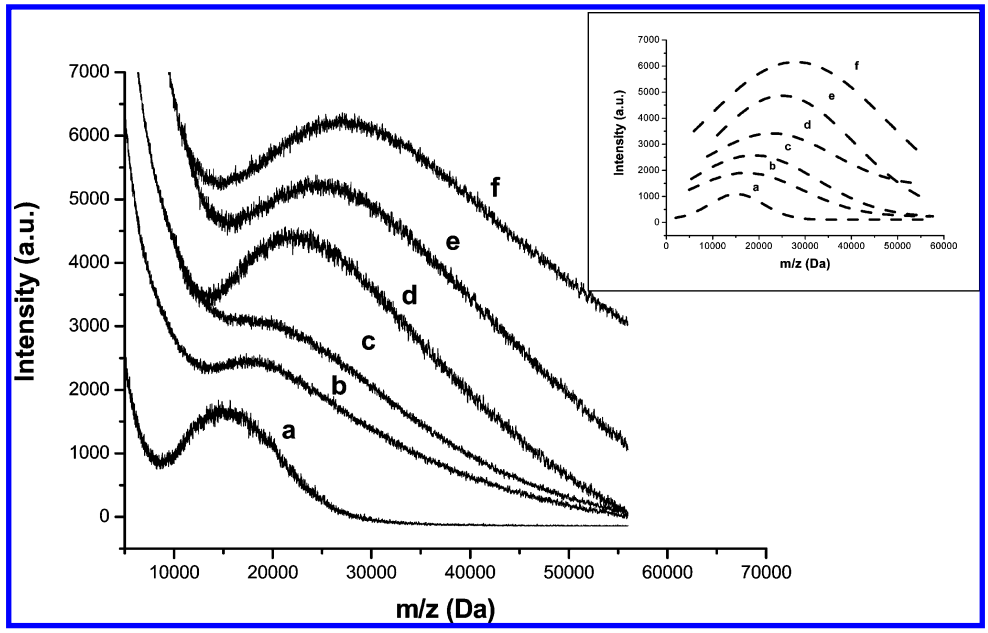

Figure 3. MALDI-TOF mass spectra of α-CD-S-AuNP synthesized with different molar ratios of α-CD-SH/Au: (a) 1:1, (b) 2:1, (c) 3:1, (d) 1:3, (e) 1:5, and (f) 1:10. The inset displays the result of the Gaussian curve fit of the mass spectra of α-CD-S-AuNP synthesized with different molar ratios of α-CD-SH/Au: (a) 1:1, (b) 2:1, (c) 3:1, (d) 1:3, (e) 1:5, and (f) 1:10.

It is evident that thiolate CD plays a critical role in controlling the size as well as the stability of AuNP. α-CD comprises torus-like macrocycles built from six D-(+)-glucopyranose units, which are linked by α-1,4 bonds with classical C1 chair conformation. This geometry gives the α-CD the wider side formed by secondary 2- and 3-hydroxyl groups and the narrower side by primary 6-hydroxyl groups as shown in Figure S3. The cavity is lined by hydrogen atoms and glycosidic oxygen bridges. As a result, a ring of hydrogen bond is formed intramolecularly between the 2-hydroxyl and 3-hydroxyl groups of adjacent glucose units O(3)-H···O(2).[11] Pinjari and co-workers found that the interglucose O(2)-H···O(3′) hydrogen bonding interactions are relatively stronger than the intraglucose O(3)-H···O(2) hydrogen bonds. In α-CD, the hydrogen bonds of primary hydroxyl groups O(6)-H···O(6′) also prevail.[25] As such, interhydrogen bonds may also possibly exist between α-CD-SH molecules when their concentrations are relatively high. In a reaction mixture (α-CD-SH/Au ≥ 1) of higher α-CD-SH concentration, interhydrogen bonds between α-CD-SH molecules become dominant, and they tend to agglomerate together; as a result, less free α-CD-SHs are available to attach to the AuNP surface, and then the NP nuclei can grow freely. This explains why the AuNP grows larger with the increase in α-CD-SH/Au (≥1).

3.3. Composition of α-CD-S-AuNP. TGA of AuNP causes thermal desorption of the thiolate ligand as volatile disulfide, leaving Au as the residual mass. Thus, the attached ligand component can be measured in relation to weight loss and residual Au core mass. Figure S4 displays the TGA data of α-CD-S-AuNP samples synthesized with 1:1, 2:1, 3:1, 1:3, 1:5, and 1:10 α-CD-SH/Au. The weight losses are 33, 23, 22, 18, 11, and 7.0%, respectively, which are consistent with the literature showing that smaller NPs have larger ligand mass fractions.[26] Their corresponding onset thermal desorption temperatures are 285, 275, 271, 265, 259, and 253 °C, respectively, demonstrating that smaller NPs possess higher thermal desorption temperatures and ligands attached to larger metal core are easier to desorb. These results are in agreement with the decrease in desorption temperature when the Au core diameter increases.[15] Collectively, these data further infer that α-CD-SH/Au < 1 will harvest larger core-sized α-CD-S-AuNPs whereas α-CD-SH/Au ≥ 1 will yield small α-CD-S-AuNPs.

More recently, MS is a valuable tool in identifying the core mass of AuNPs. Careful studies on high-resolution MS by Murray, Tsukuda, and Whetten[27] have unraveled the molecular formulas of AuNPs. Figure 3 displays the MS of α-CD-S-AuNP samples synthesized with 1:1, 2:1, 3:1, 1:3, 1:5, and 1:10 α-CD-SH/Au. Compared to the earlier work,[27] our peaks lack fine structures. All the spectra exhibit a single and broad spectral feature, which is similar to other work of large core size AuNPs[8c] and platinum NPs.[28] This can be explained by the fact that the as-synthesized α-CD-S-AuNPs are not completely monodisperse. Clearly, the major *m*/*z* peaks of the α-CD-S-AuNP samples follow the trend α-CD-SH/Au 1:1 < 2:1 < 3:1 < 1:3 < 1:5 < 1:10. To verify the average mass of these α-CD-S-AuNPs, a Gaussian curve-fit program was employed to plot the MS as depicted in the inset of Figure 3. The results demonstrate that our MS follows well with the Gaussian distribution behavior and is consistent with the literature.[28] The largest abundances of AuNPs formed are *m*/*z* 15.95, 18.04, 20.99, 22.57, 26.69, and 28.52 kDa, respectively. The average composition of α-CD-S-AuNP in terms of empirical formula $Au_x(\alpha\text{-CD-S})_y$ with the largest abundance can be determined by TGA and MS data. For AuNP synthesized with 1:1 α-CD-SH/Au and an average diameter of 1.4 ± 0.5 nm, the composition is mainly $Au_{54\pm1}(\alpha\text{-CD-S})_{5\pm1}$, which is in agreement with a previous work that Au_{55} corresponds to an average diameter of 1.4 nm.[29] The other α-CD-S-AuNPs synthesized with 2:1, 3:1, 1:3, 1:5, and 1:10 α-CD-SH/Au are $Au_{70\pm1}(\alpha\text{-CD-S})_{4\pm1}$, $Au_{83\pm1}(\alpha\text{-CD-S})_{4\pm1}$, $Au_{94\pm1}(\alpha\text{-CD-S})_{4\pm1}$, $Au_{120\pm1}(\alpha\text{-CD-S})_{3\pm1}$, and $Au_{134\pm1}(\alpha\text{-CD-S})_{2\pm1}$, respectively.

To verify the accuracy of the above findings, AAS was carried out to determine the Au content in α-CD-S-AuNP samples. The detailed procedure is described in the Supporting Information. AAS is commonly used to determine the relative compositions of the organic monolayer and the core−shell of AuNPs. The Au weight percentages of α-CD-S-AuNPs confirmed by our AAS were 63.6, 73.0, 76.0, 76.6, 83.3, and 90.0% for $Au_{54\pm1}$(α-

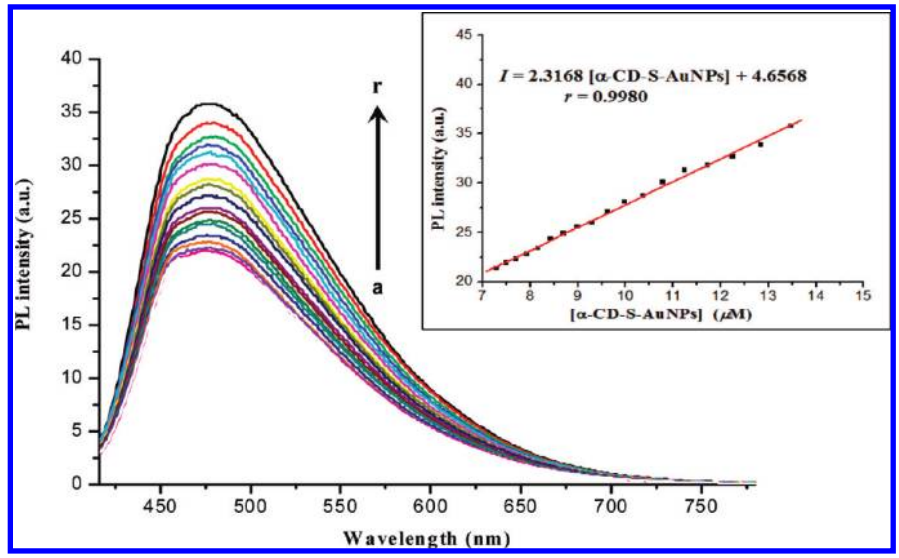

Figure 4. PL spectra of various concentrations of 1.4 nm-sized α-CD-S-AuNP: (a) 7.29, (b) 7.49, (c) 7.70, (d) 7.93, (e) 8.17, (f) 8.42, (g) 8.70, (h) 8.99, (i) 9.30, (j) 9.63, (k) 9.98, (l) 10.4, (m) 10.8, (n) 11.2, (o) 11.7, (p) 12.3, (q) 12.9, and (r) 13.5 μM. The inset displays the linear relationship between the PL intensity at excitation/emission wavelengths of 400/478 nm and the concentration of α-CD-S-AuNP.

CD-S)$_{5\pm1}$, $Au_{70\pm1}$(α-CD-S)$_{4\pm1}$, $Au_{83\pm1}$(α-CD-S)$_{4\pm1}$, $Au_{94\pm1}$(α-CD-S)$_{4\pm1}$, $Au_{120\pm1}$(α-CD-S)$_{3\pm1}$, and $Au_{134\pm1}$(α-CD-S)$_{2\pm1}$, respectively. The results are in complete agreement with the TGA and MS data. To our surprise, the number of perthiolate ligands (α-CD-SHs) attached to the Au core of NP is much smaller than that of monothiolate ligands (RSH), attributing to the fact that one single polythiolate ligand can simultaneously bind to several Au atoms of a single NP. Unfortunately, it is still not clearly understood why the number of α-CD-S ligand decreases moderately with the increase in Au atoms of our AuNPs. However, it can be postulated that the outer diameter (1.5 nm) of α-CD is too large for small AuNPs (<2.0 nm) to simultaneously accommodate several surface-attached α-CD ligands due to steric hindrance from the close proximity of the α-CD ligands.[27b,c,30] Thus, it is probable that the α-CD ligands preferably bind to the small AuNPs via the -SR-Au-SR-, -SR-Au-SR-Au-SR-, or -SR-Au-SR-Au-SR-Au-SR- staple motifs.[31] When the AuNPs are large enough, several α-CD ligands can then directly bind to one Au core through the multi-SH moiety. In other words, the surface-attached α-CD ligands are most likely to transform from the monolayer protecting (poly)ligands (with some staple motif structure) to single protecting thiolate ligands[27b] with increased α-CD-S-AuNP particle size.

3.4. PL Properties of α-CD-S-AuNP. It has been reported that AuNPs possess size-dependent PL behavior, and their PL is attributed to transitions between the filled $5d^{10}$ band and $6sp^1$ conduction band of the Au atom.[32] As such, the PL properties of our small α-CD-S-AuNPs were investigated. All the α-CD-S-AuNPs synthesized with α-CD-SH/Au 1:1, 2:1, and 3:1 in DMSO display strong blue emissions when excited at 400 nm (Figure S5). The possibility of emission arising from adventitious impurity of the reagents or synthesis was carefully scrutinized. None of the solutions including α-CD-SH used in the whole synthetic process exhibited fluorescence emission. Overall, there is firm evidence that the emission originates from α-CD-S-AuNPs itself. Our small-sized α-CD-S-AuNPs display strong blue light emission at 478 nm, which is similar to other AuNPs reported in the literature.[33] In contrast, no observable PL properties were identified for α-CD-S-AuNPs of larger core size (>2.0 nm). Among the small α-CD-S-AuNPs studied, the 1.4 nm-sized α-CD-S-AuNP produces stronger PL intensity as a result of the lower density of energy states and electronic states present in the smaller AuNPs, which probably minimize the number of internal nonradiative relaxation pathways.[34] Therefore, the 1.4 nm-sized α-CD-S-AuNP was chosen for further investigation. To ensure that the emission band is indeed PL signals from the α-CD-S-AuNP, the emission spectra at various concentrations (7.29−13.5 μM) of the 1.4 nm-sized α-CD-S-AuNP were acquired and displayed in Figure 4. No observable shift in the emission band is found. In addition, the PL intensity is linearly related to the concentration of α-CD-S-AuNP (inset of Figure 4), inferring that α-CD-S-AuNPs can disperse well in solvent. These results further demonstrate the potential of the PL properties of small core size metal NPs, especially those smaller than 2.0 nm, for luminescence sensing.

3.4.1. Enhancement Effect of Tetraalkylammonium Ion. Most attention has been focused on the investigation of chromophore−AuNP composites where AuNPs always act as photoluminescent quenchers to quench the molecular excitation energy.[16,35] However, the aggregation-enhanced emission phenomenon attracts more and more attention in chromophore−AuNPs and other organic NPs in recent years.[36] This phenomenon can be explained by the fact that the energy relaxation processes through nonradiant channels are blocked by the restriction of intramolecular motions in the aggregate state. As a result, the energy relaxes through the radiant pathway and the emission of this kind of compound is enhanced. In our pervious work, we successfully induced the linking of our α-CD-S-AuNPs by Bu_4N^+ ion.[37] Figure 5 depicts the PL spectra of α-CD-S-AuNPs as a function of the concentration of Bu_4N^+. It is observed that the emission intensity increases successively with the increasing concentration of Bu_4N^+. It has been reported that the formation of β-CD-modified AuNP assemblies is directed by the host−guest interaction of the surface-attached CDs on AuNPs and a triangular shape osmium complex.[38] Since each Bu_4N^+ carries four butyl chains, the butyl chains can enter the hydrophobic cavities of different α-CD-S-AuNPs with a concomitant effect of linking the α-CD-S-AuNPs together. This linkage restricts the intramolecular vibration of α-CD-S-AuNPs, thus minimizing the number of internal nonradiative relaxation pathways. In addition, the PL enhancement of other tetraalkylammonium ions with different carbon chain lengths on the PL of α-CD-S-AuNPs was investigated and is depicted in the inset of Figure 5. The PL enhancement effect (%) is defined as

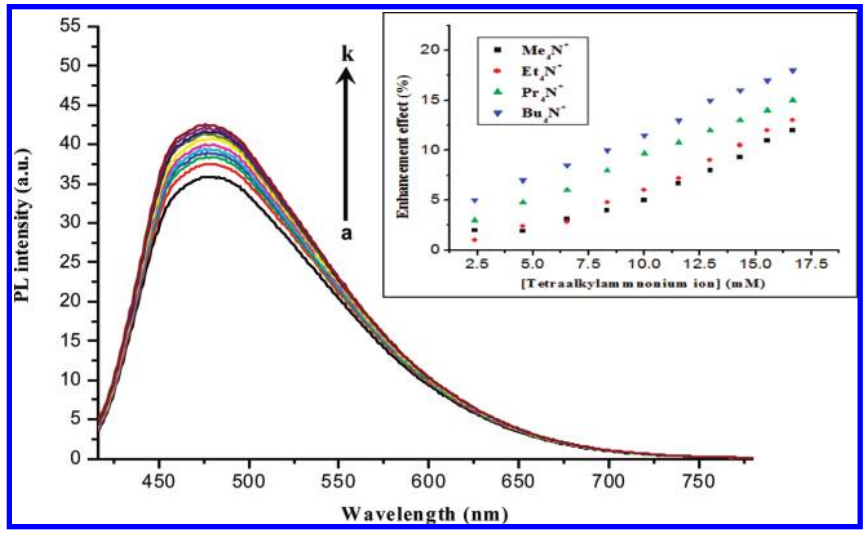

Figure 5. PL enhancement effect of tetrabutylammonium ion on 1.4 nm-sized α-CD-S-AuNP (13.5 μM): (a) 0.00, (b) 2.38, (c) 4.55, (d) 6.52, (e) 8.33, (f) 10.0, (g) 11.5, (h) 12.9, (i) 14.3, (j) 15.5, and (k) 16.7 mM Bu_4N^+. The inset displays the relationship between the PL enhancement effect at excitation/emission wavelengths of 400/478 nm and the concentration of various tetraalkylammonium ions (Me_4N^+, Et_4N^+, Pr_4N^+, and Bu_4N^+).

$[(I - I_o)/I_o]$ where I_o and I are the PL intensity in the absence and presence of tetraalkylammonium ion, respectively. The enhancement effect follows the trend $Bu_4N^+ > Pr_4N^+ > Et_4N^+ \approx Me_4N^+$, indicating the possible formation of inclusion complexes between the α-CD-S-AuNPs and the larger enhancement effect for the longer carbon chain length tetraalkylammonium ions. This aggregation-enhanced emission phenomenon is consistent with our pervious report[37] and is useful for these types of AuNPs, which have potential applications in optical sensing tetraalkylammonium ions.

3.4.2. Quenching Effect of Mercury(II) Ion. Mercury is one of the toxic heavy metals and it exists in metallic, inorganic and organic forms. Hg(II) ion, the most stable inorganic form of Hg, is a caustic and carcinogenic species and possesses high cellar toxicity even at low concentrations.[39] These problems have prompted researchers to develop efficient and sensitive methods for trace analysis of Hg(II) in the environment. Besides conventional methods, nanosensors based on AuNPs[16,34,35] and semiconductor quantum dots (QDs)[40] have attracted considerable interest in recent years. Herein, we demonstrate a highly sensitive and selective method for ultratrace determination of Hg(II) based on PL quenching on small α-CD-S-AuNPs.

Figure 6 displays the PL emission spectra of α-CD-S-AuNPs as a function of the concentration of Hg(II) from 0.00 to 26.4 nM. The observed PL intensity centered at 478 nm (excitation 400 nm) gradually decreases with increasing concentration of Hg(II) and there is no optical shift of PL emission band. The PL intensity is almost completely quenched at 33.7 nM (Figure S6A). The PL quenching of α-CD-S-AuNPs is achieved through facilitating nonradiative electron relaxation process from α-CD-S-AuNPs to Hg(II). This effect can be employed to develop a PL quenching method for the determination of Hg(II). Figure 7 displays the Stern−Volmer plot of I_o/I versus [Hg(II)], where I_o and I are the PL intensity in the absence and presence of Hg(II), respectively. The curve displays good linear relationship at a low concentration range (0.0962−10.0 nM) of Hg(II) as shown in the inset of Figure 7. However, it turns to a step upward curvature at higher Hg(II) concentration (>10.0 nM), indicating that the quenching of α-CD-S-AuNPs is more effective at higher Hg(II) concentration. Both dynamic and static quenching seem to act together, suggesting a more complex quenching model (*vide infra*). Electron transfer and ion-binding

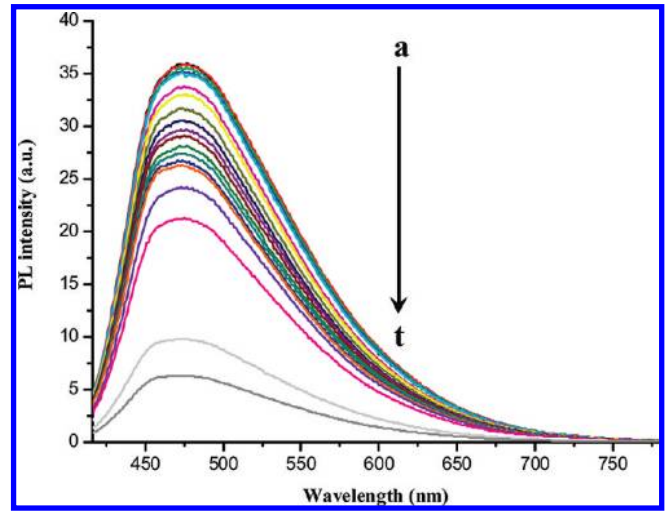

Figure 6. PL of 1.4 nm-sized α-CD-S-AuNP (13.5 μM) in the presence of various concentrations of Hg(II): (a) 0.00, (b) 0.0962, (c) 0.337, (d) 0.524, (e) 0.637, (f) 0.962, (g) 1.84, (h) 2.64, (i) 3.37, (j) 4.04, (k) 4.66, (l) 5.24, (m) 5.77, (n) 6.27, (o) 6.73, (p) 9.62, (q) 13.2, (r) 18.4, (s) 23.3, and (t) 26.4 nM. The PL intensity was monitored at excitation/emission wavelengths of 400/478 nm.

can possibly lead to the decrease of PL emission with the former playing an important role.[40b,c] The limit of detection (LOD) based on the 3σ at the blank is 49 pM (9.7 ppt), which is much lower than the maximum level (2.0 ppb) of Hg in drinking water permitted by the U.S. Environmental Protection Agency (EPA). The relative standard derivation for six replicate measurements of a 3.37 nM Hg(II) solution is 1.29%. Our approach can develop an ultrasensitive α-CD-S-AuNP-based nanosensor for the determination of Hg(II).

Moreover, it was observed that the α-CD-S-AuNPs solution would change from colorless to light red in the presence of micromolar concentration of Hg(II). The PL emission spectrum of α-CD-S-AuNPs is hypsochromically shifted under higher concentrations of Hg(II) as depicted in Figure S6A. It is possible that dynamic quenching of α-CD-S-AuNPs is dominant under low concentration of Hg(II) (<10 nM). When the concentration of Hg(II) increases, both dynamic and static quenching come to play a dominant role, leading to the upward curvature of the

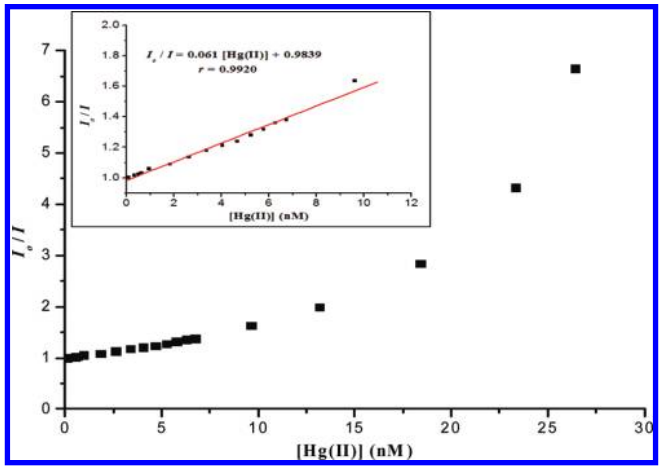

Figure 7. Stern−Volmer plot of I_o/I against [Hg(II)]. The inset displays the linear relationship of the Stern−Volmer plot at the low concentration range (0.0962−10.0 nM) of Hg(II). I_o and I are the PL intensities of α-CD-S-AuNP at excitation/emission wavelengths of 400/478 nm in the absence and presence of Hg(II), respectively.

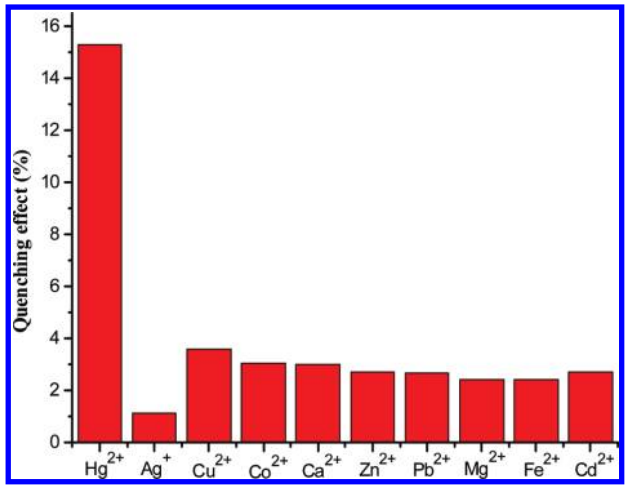

Figure 8. The quenching effect of various metal ions on 1.4 nm-sized α-CD-S-AuNPs (13.5 μM). The concentration of all metal ions except Hg^{2+} and Ag^{+} (3.37 nM) are 3.37 μM. The PL intensity was monitored at excitation/emission wavelengths of 400/478 nm.

Stern−Volmer plot (Figure 7). This conclusion is supported by the UV−vis absorption spectra of α-CD-S-AuNPs with Hg(II) as depicted in the inset of Figure S6A. The UV−vis absorption spectrum does not change in the presence of 0.00−10.0 nM Hg(II). By contrast, the absorption increases drastically when there is 23.1 μM Hg(II), possibly attributing to the formation of larger Au-HgNPs, i.e., deposition of Hg(II) onto AuNPs, resulting in an increase of the absorption intensity in UV−vis absorption spectrum of AuNPs. By contrast, α-CD does not show any PL regardless of Hg(II), as shown in Figure S6B, inferring that the AuNPs indeed play an importance role in determining the PL properties of α-CD-S-AuNPs.

Finally, to test the selectivity of our proposed PL α-CD-S-AuNP-based quenching method, the PL emission responses in the presence of various metal ions including Hg^{2+}, Ag^{+}, Cu^{2+}, Co^{2+}, Ca^{2+}, Zn^{2+}, Pb^{2+}, Mg^{2+}, Fe^{2+}, and Cd^{2+} at a concentration of 3.37 μM (except Hg^{2+} and Ag^{+} at 3.37 nM), 1000 times greater than that of Hg^{2+}, were studied and plotted in Figure 8. The quenching effect (%) is defined as $[(I_o - I)/I_o]$, where I_o and I are the PL intensity in the absence and presence of metal ion, respectively. It is evident that high concentrations of other ions do not produce any noticeable effect on the emission signals of α-CD-S-AuNPs as compared to $[Hg^{2+}]$. Hence, our as-prepared α-CD-S-AuNPs should show excellent selectivity for ultratrace determination of Hg(II) in the nanomolar range.

4. Conclusion

Our work demonstrates that the molar ratio of α-CD-SH/Au plays a predominant role in controlling the core size of α-CD-S-AuNP. When α-CD-SH/Au is ≥1, small α-CD-S-AuNPs (Au core <2.0 nm) will be harvested, and their core size increases with the increase in α-CD-SH/Au. It is postulated that the interhydrogen bonds of α-CD-SH ligands reduce their availability for binding to the Au nuclei, thus allowing embryonic AuNPs to grow into larger sizes. By contrast, when α-CD-SH/Au is controlled at <1, α-CD-S-AuNPs of diameter larger than 2.5 nm are formed, and their core size increases with the decrease in α-CD-SH/Au, attributing to the fact that AuNPs tend to grow larger due to the decrease in free α-CD-SH ligands for stabilizing the AuNPs. The smallest α-CD-S-AuNP of 1.4 nm core diameter is acquired at 1:1 α-CD-SH/Au. All α-CD-S-AuNPs of core diameters smaller than 2.0 nm possess strong PL properties, which are in contrast to the larger ones. It is observed for the first time that tetraalkylammonium ions can enhance the PL of α-CD-S-AuNPs via the formation of a rigid α-CD-S-AuNPs network. Since traalkylammonium ion is able to form inclusion complexes with α-CD-S-AuNPs in the hydrophobic cavities of the surface-attached thiolated α-CD, it can induce the interlinkage of α-CD-S-AuNPs. Finally, it was determined that the 1.4 nm-sized α-CD-S-AuNPs can be applied for PL sensing Hg(II). The sensitivity of α-CD-S-AuNPs to Hg(II) is very high, and the LOD can be as low as 49 pM. It also possesses remarkable selectivity over other metal ions. Our nontoxic α-CD-S-AuNPs are especially beneficial as compared to the commonly used semiconductor QDs that contain toxic metals. This important feature will pave the way for ultrasensitive detection of Hg(II) using α-CD-S-AuNPs.

Acknowledgment. M.C.P. acknowledges the receipt of a postgraduate studentship from the Additional UGC-funded Research Postgraduate Places in the area of Environmental and Human Health Risk Assessment of Persistent Toxic Substance. We would express our sincere thanks to Ms. Silvia T. Mo of the Department of Chemistry, Hong Kong Baptist University, for acquiring the MALDI-TOF MS, Mr. T. F. Hung of the Department of Physics and Materials Science, City University of Hong Kong, for taking the TEM images of AuNP samples, and Mr. K. M. Ho of the Department of Materials Characterization and Preparation Facility, Hong Kong University of Science and Technology, for taking the HRTEM images of AuNP samples. The work described in this paper was supported by a grant from the Research Grants Council of the Hong Kong Special Administrative Region, China (Project No. HKBU 2006/06P). This work will be presented at The 17th Symposium on Chemistry Postgraduate Research in Hong Kong on 24 April 2010.

Supporting Information Available: The syntheses of per-6-iodo-α-cyclodextrin and per-6-thio-α-cyclodextrin, AAS analysis, IR spectra, TEM images and TGA of α-CD-S-AuNPs, and PL spectra and UV−vis spectra of α-CD-S-AuNPs in the presence of higher concentrations of Hg(II). This material is available free of charge via the Internet at http://pubs.acs.org.

References and Notes

(1) (a) Souza, G. R.; Miller, J. H. *J. Am. Chem. Soc.* **2001**, *123*, 6734–6735. (b) Palui, G.; Ray, S.; Banerjee, A. *J. Mater. Chem.* **2009**, *19*, 3457–3468.

(2) (a) Brust, M.; Walker, M.; Bethell, D.; Schiffrin, D. J.; Whyman, R. *J. Chem. Soc., Chem. Commun.* **1994**, 801–802. (b) Agasti, S. S.; You, C.-C.; Arumugam, P.; Rotello, V. M. *J. Mater. Chem.* **2008**, *18*, 70–73.

(3) (a) Akamatsu, K.; Deki, S. *J. Mater. Chem.* **1997**, *7*, 1773–1777. (b) Templeton, A. C.; Wuelfing, W. P.; Murray, R. W. *Acc. Chem. Res.* **2000**, *33*, 27–36.

(4) Zamborini, F. P.; Hicks, J. F.; Murray, R. W. *J. Am. Chem. Soc.* **2000**, *122*, 4514–4515.

(5) (a) Sayo, K.; Deki, S.; Hayashi, S. *J. Mater. Chem.* **1999**, *9*, 937–942. (b) Eklund, S. E.; Cliffel, D. E. *Langmuir* **2004**, *20*, 6012–6018. (c) Zhou, X.; Xu, W.; Liu, G.; Panda, D.; Chen, P. *J. Am. Chem. Soc.* **2010**, *132*, 138–146.

(6) Daniel, M.-C.; Astruc, D. *Chem. Rev.* **2004**, *104*, 293–346.

(7) Templeton, A. C.; Chen, S.; Gross, S. M.; Murray, R. W. *Langmuir* **1999**, *15*, 66–76.

(8) (a) Choi, M. M. F.; Dougles, A. D.; Murray, R. W. *Anal. Chem.* **2006**, *78*, 2779–2785. (b) Lo, C. K.; Paau, M. C.; Xiao, D.; Choi, M. M. F. *Anal. Chem.* **2008**, *80*, 2439–2446. (c) Zhang, Y.; Shuang, S.; Dong, C.; Lo, C. K.; Paau, M. C.; Choi, M. M. F. *Anal. Chem.* **2009**, *81*, 1676–1685.

(9) Lo, C. K.; Xiao, D.; Choi, M. M. F. *J. Mater. Chem.* **2007**, *17*, 2418–2427.

(10) (a) Keita, B.; Biboum, R. N.; Mbomekallé, I. M.; Floquet, S.; Simonnet-Jégat, C.; Cadot, E.; Miserque, F.; Berthet, P.; Nadjo, L. *J. Mater. Chem.* **2008**, *18*, 3196–3199. (b) Kanehara, M.; Takahashi, H.; Teranishi, T. *Angew. Chem., Int. Ed.* **2008**, *47*, 307–310. (c) Ohyama, J.; Hitomi, Y.; Higuchi, Y.; Shinagawa, M.; Mukai, H.; Kodera, M.; Teramura, K.; Shishido, T.; Tanaka, T. *Chem. Commun.* **2008**, 6300–6302.

(11) Li, S.; Purdy, W. C. *Chem. Rev.* **1992**, *92*, 1457–1470.

(12) (a) Rojas, M. T.; Königer, R.; Stoddart, J. F.; Kaifer, A. E. *J. Am. Chem. Soc.* **1995**, *117*, 336–343. (b) Crespo-Biel, O.; Dordi, B.; Maury, P.; Péter, M.; Reinhoudt, D. N.; Huskens, J. *Chem. Mater.* **2006**, *18*, 2545–2551. (c) Park, C.; Youn, H.; Kim, H.; Noh, T.; Kook, Y. H.; Oh, E. T.; Park, H. J.; Kim, C. *J. Mater. Chem.* **2009**, *19*, 2310–2315. (d) Perl, A.; Kumprecht, L.; Kraus, T.; Armspach, D.; Matt, D.; Reinhoudt, D. N.; Huskens, J. *Langmuir* **2009**, *25*, 1534–1539.

(13) (a) Liu, J.; Mendoza, S.; Román, E.; Lynn, M. J.; Xu, R.; Kaifer, A. E. *J. Am. Chem. Soc.* **1999**, *121*, 4304–4305. (b) Liu, J.; Alvarez, J.; Ong, W.; Román, E.; Kaifer, A. E. *J. Am. Chem. Soc.* **2001**, *123*, 11148–11154.

(14) Liu, J.; Ong, W.; Román, E.; Lynn, M. J.; Kaifer, A. E. *Langmuir* **2000**, *16*, 3000–3002.

(15) Hostetler, M. J.; Wingate, J. E.; Zhong, C.-J.; Harris, J. E.; Wachet, R. W.; Clark, M. R.; Londono, J. D.; Green, S. J.; Stokes, J. J.; Wignall, G. D.; Glish, G. L.; Porter, M. D.; Evans, N. D.; Murray, R. W. *Langmuir* **1998**, *14*, 17–30.

(16) Zhang, A.; Chen, J.; Wu, G.; Wei, H.; He, C.; Kai, X.; Wu, G.; Chen, Y. *Microchim. Acta* **2009**, *164*, 17–27.

(17) (a) Bratu, I.; Astilean, S.; Ionesc, C.; Indrea, E.; Huvenne, J. P.; Legrand, P. *Spectrochim. Acta, Part A* **1998**, *54*, 191–196. (b) Wei, M.; Wang, J.; He, J.; Evans, D. G.; Duan, X. *Microporous Mesoporous Mater.* **2005**, *78*, 53–61. (c) Liu, Y.; Zhao, Y. L.; Chen, Y.; Wang, M. *Macromol. Rapid Commun.* **2005**, *26*, 401–406. (d) Diao, G.; Qian, C.; Chen, M.; Huang, Y. *Supramol. Chem.* **2006**, *18*, 117–123. (e) Na, N.; Hu, Y.; Ouyang, J.; Baeyens, W. R. G.; Delanghe, J. R.; Taes, Y. E. C.; Xie, M.; Chen, H.; Yang, Y. *Talanta* **2006**, *69*, 866–872.

(18) Negishi, Y.; Nobusada, K.; Tsukuda, T. *J. Am. Chem. Soc.* **2005**, *127*, 5261–5270.

(19) Underwood, S.; Mulvaney, P. *Langmuir* **1994**, *10*, 3427–3430.

(20) (a) Driskell, J. D.; Lipert, R. J.; Porter, M. D. *J. Phys. Chem. B* **2006**, *110*, 17444–17451. (b) Amendola, V.; Meneghetti, M. *J. Phys. Chem. C* **2009**, *113*, 4277–4285. (c) Sakamoto, M.; Tachikawa, T.; Fujitsuka, M.; Majima, T. *Langmuir* **2009**, *25*, 13888–13893.

(21) Liu, J.; Alvarez, J.; Ong, W.; Kaifer, A. E. *Nano Lett.* **2001**, *1*, 57–60.

(22) Liu, Y.; Male, K. B.; Bouvrette, P.; Luong, J. H. T. *Chem. Mater.* **2003**, *15*, 4172–4180.

(23) Kabashin, A. V.; Meunier, M.; Kingston, C.; Luong, J. H. T. *J. Phys. Chem. B* **2003**, *107*, 4527–4531.

(24) Leff, D. V.; Ohara, P. C.; Health, J. R.; Gelbart, W. M. *J. Phys. Chem.* **1995**, *99*, 7036–7041.

(25) Pinjari, R. V.; Joshi, K. A.; Gejji, S. P. *J. Phys. Chem. A* **2006**, *110*, 13073–13080.

(26) Luo, J.; Maye, M. M.; Han, L.; Kariuki, N. N.; Jones, V. W.; Lin, Y.; Engelhard, M. H.; Zhong, C.-J. *Langmuir* **2004**, *20*, 4254–4260.

(27) (a) Schaaff, T. G.; Knight, G.; Shafigullin, M. N.; Borkman, R. F.; Whetten, R. L. *J. Phys. Chem. B* **1998**, *102*, 10643–10646. (b) Heaven, M. W.; Dass, A.; White, P. S.; Holt, K. M.; Murray, R. W. *J. Am. Chem. Soc.* **2008**, *130*, 3754–3755. (c) Chaki, N. K.; Negishi, Y.; Tsunoyama, H.; Shichibu, Y.; Tsukuda, T. *J. Am. Chem. Soc.* **2008**, *130*, 8608–8610.

(28) Navin, J. K.; Grass, M. E.; Somorjai, G. A.; Marsh, A. L. *Anal. Chem.* **2009**, *81*, 6295–6299.

(29) Turner, M.; Golovko, V. B.; Vaughan, O. P. H.; Abdulkin, P.; Berenguer-Murcia, A.; Tikhov, M. S.; Johnson, B. F. G.; Lambert, R. M. *Nature* **2008**, *454*, 981–984.

(30) Ng, C. H. B.; Yang, J.; Fan, W. Y. *J. Phys. Chem. C* **2008**, *112*, 4141–4145.

(31) (a) Jadzinsky, P. D.; Calero, G.; Ackerson, C. J.; Bushnell, D. A.; Kornberg, R. D. *Science* **2007**, *318*, 430–433. (b) Pei, Y.; Gao, Y.; Shao, N.; Zeng, X. C. *J. Am. Chem. Soc.* **2009**, *131*, 13619–13621.

(32) (a) Yang, Y.; Chen, S. *Nano Lett.* **2003**, *3*, 75–79. (b) Negishi, Y.; Tsukuda, T. *Chem. Phys. Lett.* **2004**, *383*, 161–165. (c) Lee, D.; Donkers, R. L.; Wang, G.; Harper, A. S.; Murray, R. W. *J. Am. Chem. Soc.* **2004**, *126*, 6193–6199. (d) Negishi, Y.; Takasugi, Y.; Sato, S.; Yao, H.; Kimura, K.; Tsukuda, T. *J. Am. Chem. Soc.* **2004**, *126*, 6518–6519.

(33) Liu, X.; Li, C.; Xu, J.; Lv, J.; Zhu, M.; Guo, Y.; Cui, S.; Liu, H.; Wang, S.; Li, Y. *J. Phys. Chem. C* **2008**, *112*, 10778–10783.

(34) Huang, C.-C.; Yang, Z.; Lee, K.-H.; Chang, H.-T. *Angew. Chem., Int. Ed.* **2007**, *46*, 6824–6828.

(35) (a) Chen, J.; Zheng, A.; Chen, A.; Gao, Y.; He, C.; Kai, X.; Wu, G.; Chen, Y. *Anal. Chim. Acta* **2007**, *599*, 134–142. (b) Huang, C.-C.; Chang, H.-T. *Anal. Chem.* **2006**, *78*, 8332–8338.

(36) (a) An, B.-K.; Kwon, S.-K.; Jung, S.-D.; Park, S. Y. *J. Am. Chem. Soc.* **2002**, *124*, 14410–14415. (b) Lim, S.-J.; An, B.-K.; Jung, S. D.; Chung, M. A.; Park, S. Y. *Angew. Chem., Int. Ed.* **2004**, *43*, 6346–6350. (c) Ostrowski, J. C.; Mikhailovsky, A.; Bussian, D. A.; Summers, M. A.; Buratto, S. K.; Bazan, G. C. *Adv. Funct. Mater.* **2006**, *16*, 1221–1227. (d) Li, C.; Liu, X.; Yuan, M.; Li, J.; Guo, Y.; Xu, J.; Zhu, M.; Lv, J.; Liu, H.; Li, Y. *Langmuir* **2007**, *23*, 6754–6760. (e) Lv, J.; Jiang, L.; Li, C.; Liu, X.; Yuan, M.; Xu, J.; Zhou, W.; Song, Y.; Liu, H.; Li, Y.; Zhu, D. *Langmuir* **2008**, *24*, 8297–8302. (f) Lv, J.; Zhao, Y.; Li, G.; Li, Y.; Liu, H.; Li, Y.; Zhu, D.; Wang, S. *Langmuir* **2009**, *25*, 11351–11357.

(37) Paau, M. C.; Lo, C. K.; Choi, M. M. F. *J. Chromatogr. A* **2009**, *48*, 8557–8562.

(38) Zeng, Q.; Marthi, R.; McNally, A.; Dickinson, C.; Keyes, T. E.; Forster, R. J. *Langmuir* **2010**, *26*, 1325–1333.

(39) (a) Sekowski, J. W.; Malkas, L. H.; Wei, Y.; Hickey, R. J. *Toxicol. Appl. Pharmacol.* **1997**, *145*, 268–276. (b) Zheng, W.; Aschner, M.; Ghersi-Egea, J.-F. *Toxicol. Appl. Pharmacol.* **2003**, *192*, 1–11.

(40) (a) Cai, Z.-X.; Yang, H.; Zhang, Y.; Yan, X.-P. *Anal. Chim. Acta* **2006**, *559*, 234–239. (b) Xia, Y.-S.; Zhu, C.-Q. *Talanta* **2008**, *75*, 215–221. (c) Han, B.; Yuan, J.; Wang, E. *Anal. Chem.* **2009**, *81*, 5569–5573. (d) Leng, B.; Zou, L.; Jiang, J.; Tian, H. *Sens. Actuators B* **2009**, *140*, 162–169. (e) Long, Y.; Jiang, D.; Zhu, X.; Wang, J.; Zhou, F. *Anal. Chem.* **2009**, *81*, 2652–2657.

JP101571K